IMPACT OF INSTRUMENT FOOTPRINT SIZE IN THE PRESENCE OF LOW-INDUCTION-NUMBER MATERIALS

Cathleen A. Geiger[1,2], Jesse P. Samluk[2], Chester J. Weiss[3,4]
[1] Geography, University of Delaware, Newark, DE, USA
[2] Electrical Engineering, University of Delaware, Newark, DE, USA
[3] Sandia National Laboratories, Albuquerque, NM, USA
[4] University of New Mexico, Albuquerque, NM, USA

ABSTRACT

Findings from studies exploring spatial aliasing, scaling laws, and especially waveform and filter shapes ignited a curiosity in our research team to re-examine fundamental assumptions in electromagnetic (EM) responses in the presence of sea ice as a low-induction-number material floating on top of sea water. We found that most sea ice EM studies rely on 1-D half-space algorithms so we developed interdisciplinary connections between sea ice, electrical engineering, and solid-earth geophysics. The result is the initial testing of a 3-D full-physics heterogeneous finite-volume electromagnetic induction model based on Lorenz-Gauged A-Φ Decomposition (APhiD). Here, we demonstrate some of the sensitivities identified in terms of instrument footprint size relative to conductivity properties of sea ice.

Explanation of Model Output

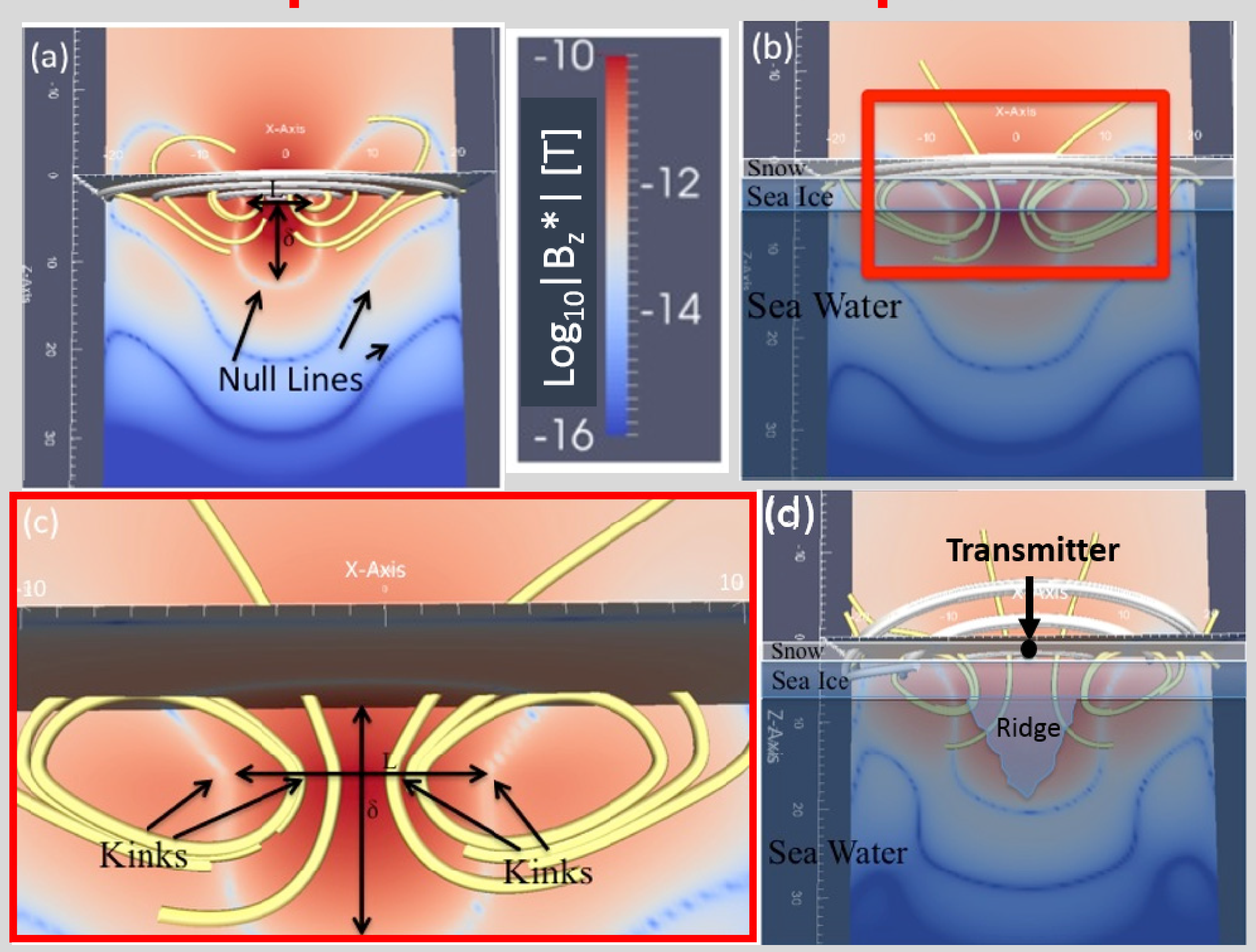

Fig. 1. Excerpts from *Samluk et al.* (2015) showing capabilities of APhiD. Each panel shows contours of logarithmically scaled magnetic flux density from the vertical direction B_z* formulated as an absolute value in log base 10. Thick "Null Lines" are locations where magnetic fields reverse polarity with strong gradients giving rise to a pulse shape *with horizontal cross section "L" denoting footprint size.* White and yellow tubular lines denote current and magnetic flux density, respectively. "Kinks" refer to bends in field lines at material boundaries of air and water (a), sea ice and water (b) with zoomed box from (b) shown in panel (c). Panel (d) shows EM responses when the transmitter is located directly over a simulated unconsolidated ridge.

Sensitivity to EM Frequencies and Transmitter Heights

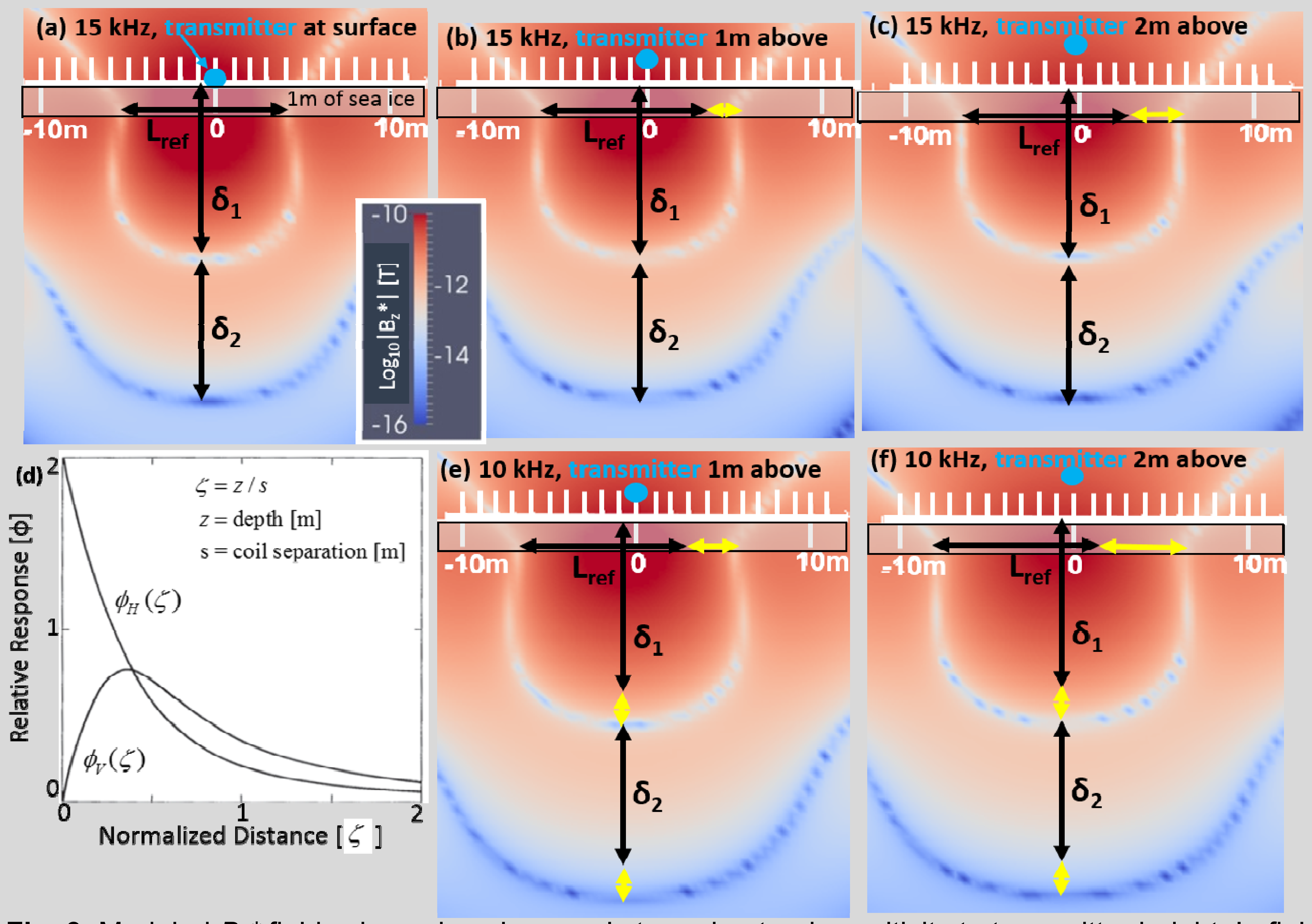

Fig. 3. Modeled B_z* fields shown in color panels to understand sensitivity to transmitter height. In field work parlance, an instrument "carry height" is defined relative to the surface set at z=0. Typical material conductivity values are used for air (equal to free permittivity), 1m thick sea ice at 0.02 S/m, and sea water at 2 S/m. Comparison between 10 and 15 kHz transmitters show differences in pulse spacing (yellow arrows) which is more compressed at higher frequency. Panel (d) shows weighted contributions (Φ_H) of material conductivities relative to distance from transmitter for horizontal (H) and vertical (V) polarization; horizontal polarization in examples shown. Hand-notated scaled references are added as visual aid to understand differences (yellow arrows) in pulse sizes. Note, in particular, the asymmetry in pulse size in the horizontal versus vertical direction **with greater sensitivity in horizontal pulse width as a surrogate for instrument footprint size.**

Footprint Sensitivity in Simple Control Runs

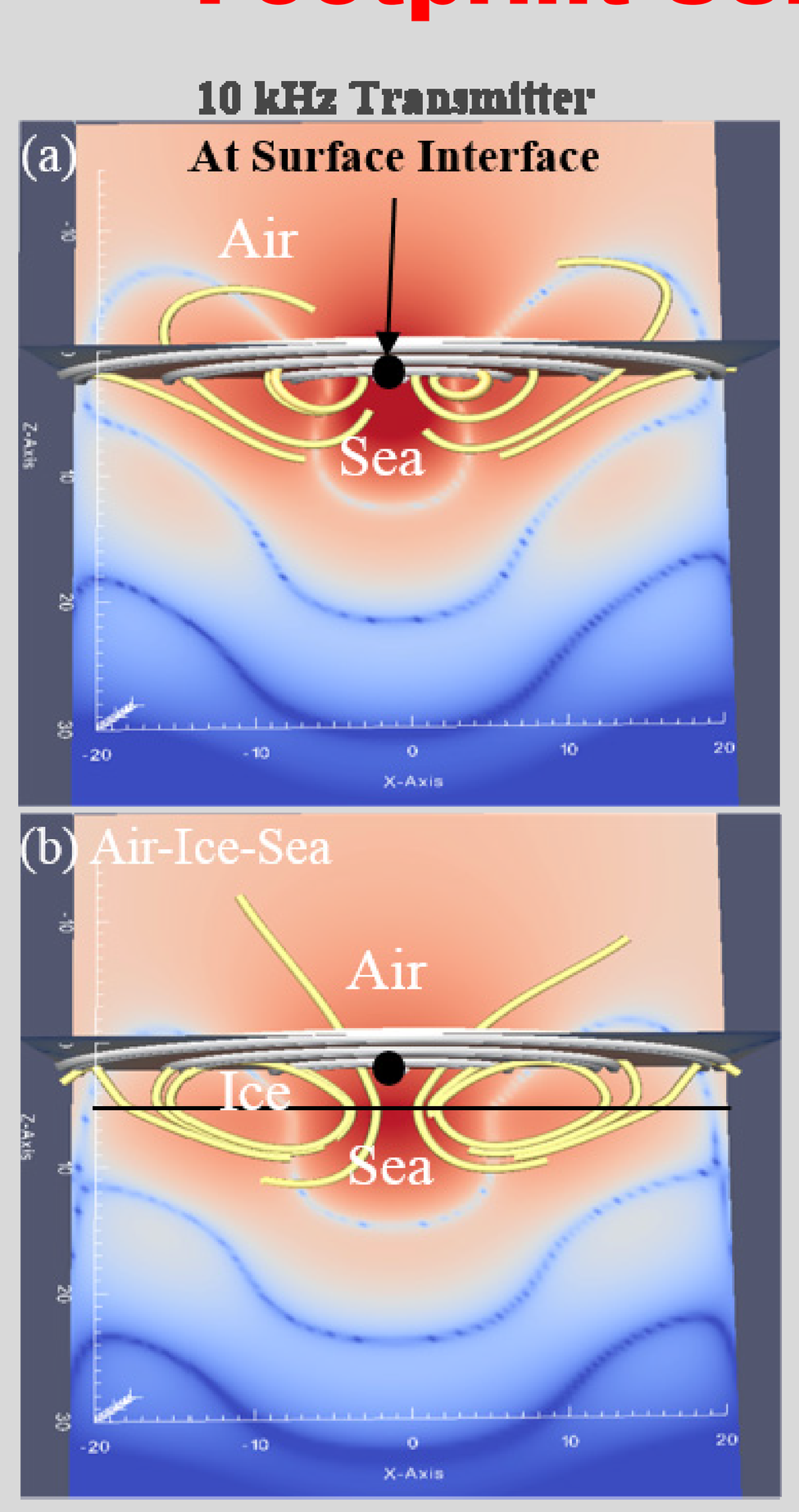

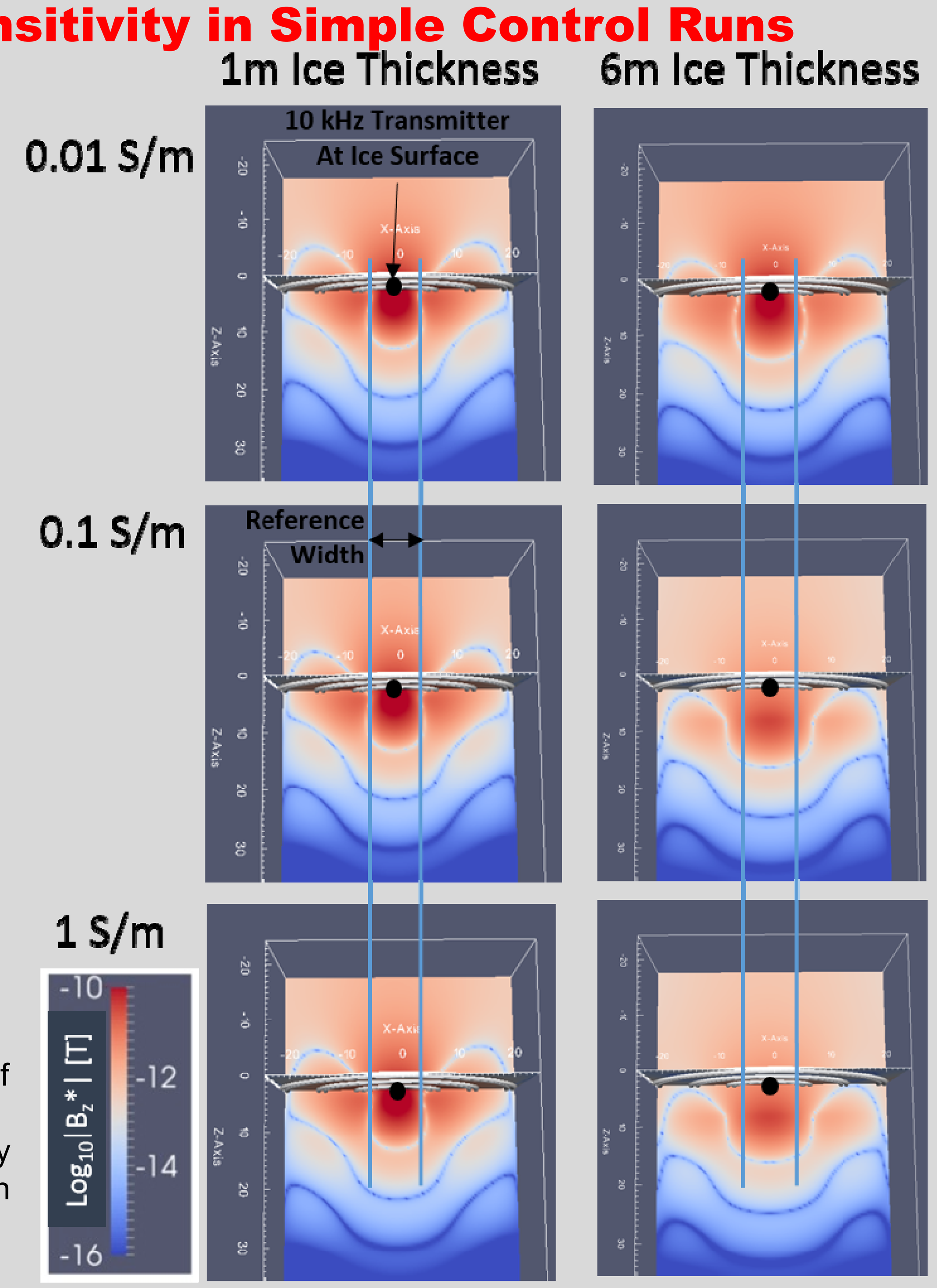

Fig. 2. Simple control runs with horizontal layers composed of uniform material conductivity values. Panel (a) is the simplest with an air-water only interface. Panel (b) includes the addition of a 3 m level sea ice layer. These and remaining six panels already show visually strong sensitivity in pulse widths depending on ice conductivity and thickness.

Sensitivity to Transmitter Placement on a Simple Ridge

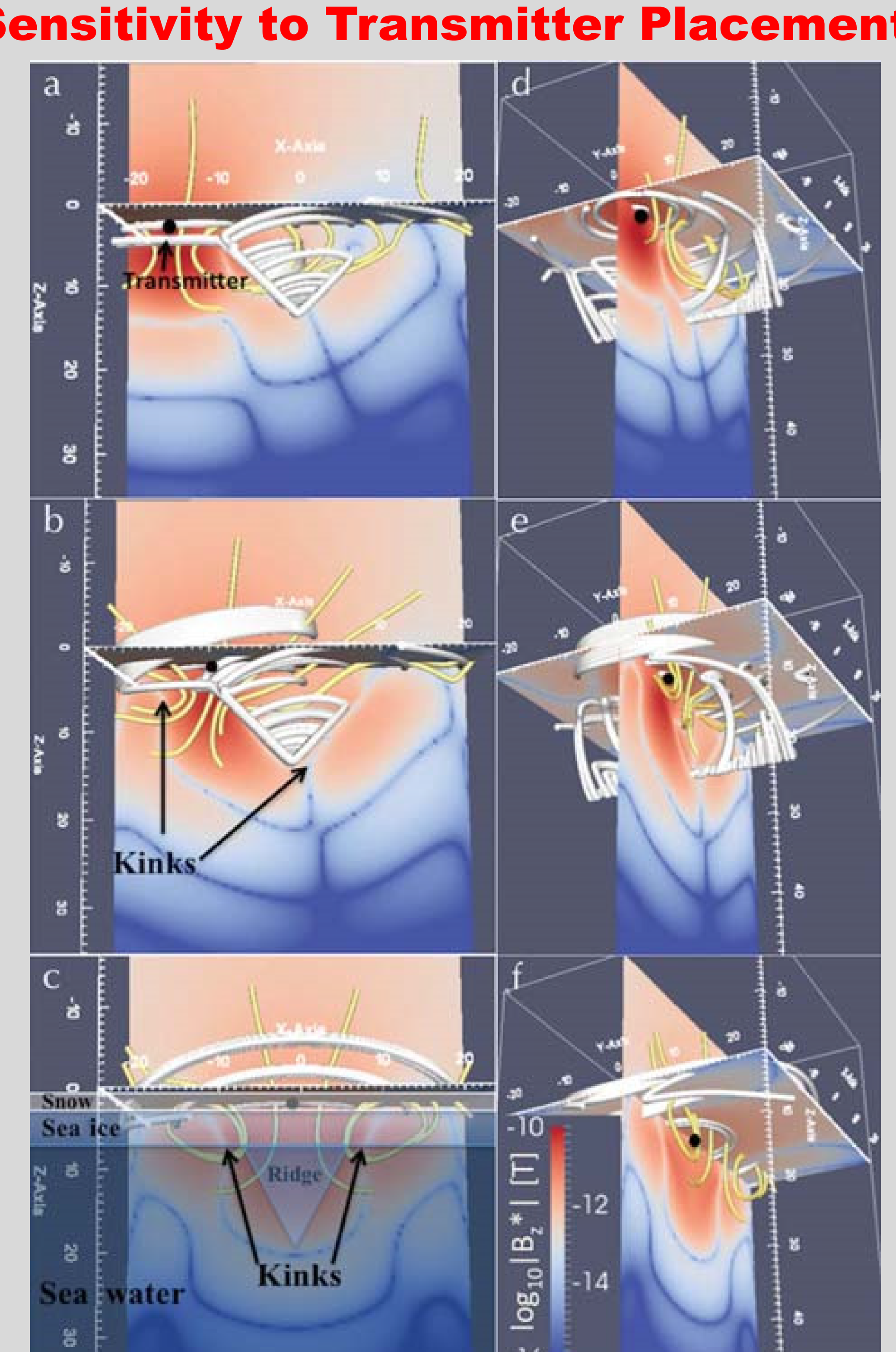

Fig. 4. Excerpt from *Samluk et al.* (2015) simulating current density lines (normalized real component), magnetic flux density lines (normalized imaginary component) and color map of the quadrature component of the magnetic flux density in logarithmic space for a multiyear ice (MY) ridge, using Haas and Druckenmiller (2009) values (0.020 S m⁻¹ for both level and ridged ice). This configuration has air, 0.5m of snow, 3m of level sea ice, a MY ridge, and sea water. The transmitter loop is shown as a black 'source' dot. In (c), the layers of snow, sea ice, sea water and an ice ridge are labeled for clarity. Field line results are shown from two perspectives with source at three locations to show how scattered the signals become as they approach a ridge due to refraction and physiographic interference based on the Huygens–Fresnel principle. Refraction is where the EM waves 'bend' the envelope of a spherical wave into a new wave front via superposition. The only time that these patterns do not occur is when the transmitter is above the ridge apex, in which case ridge symmetry matches the field shape.

Sandia National Laboratories is a multi-program laboratory managed and operated by Sandia Corporation, a wholly owned subsidiary of Lockheed Martin Corporation, for the U.S. Department of Energy's National Nuclear Security Administration under contract DE-AC04-94AL85000.

Model Explanation

The APhiD model essentially works like a transmitter-receiver pair with three very important distinctions. Firstly, we can place one or many transmitters anywhere within the model domain. Secondly, every grid cell is a receiver. Thirdly, and subsequently, we can visualize the steady state shape of current density lines and magnetic field lines to gain deeper insight into the shape of EM fields based on prescribed material thicknesses and associated material conductivities. Essentially, at any prescribed location, the apparent conductivity can be calculated as a scaled ratio between transmitter value and receiver value at each given location to make direct comparisons between field instruments and numerical simulations. The added advantage of the model is an ability to see all the locations at once as a potential planning tool for field work observations as well as calibration and validation of EM responses from airborne instruments.

Insight from Multiple Transmitter Interactions

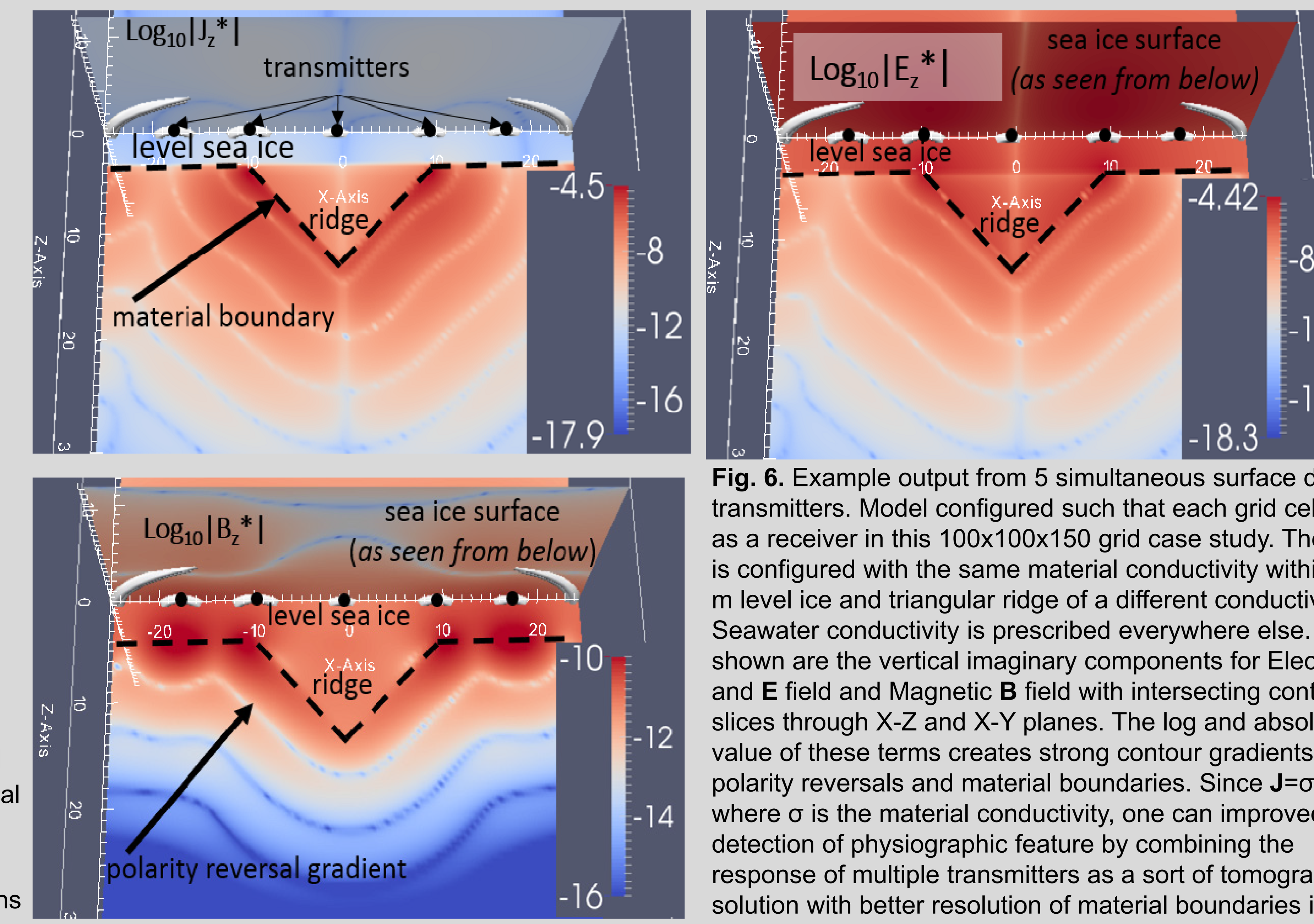

Fig. 6. Example output from 5 simultaneous surface dipole transmitters. Model configured such that each grid cell acts as a receiver in this 100x100x150 grid case study. The study is configured with the same material conductivity within the 3 m level ice and triangular ridge of a different conductivity. Seawater conductivity is prescribed everywhere else. Terms shown are the vertical imaginary components for Electric **J** and **E** field and Magnetic **B** field with intersecting contoured slices through X-Z and X-Y planes. The log and absolute value of these terms creates strong contour gradients at polarity reversals and material boundaries. Since **J**=σ**E**, where σ is the material conductivity, one can improved detection of physiographic feature by combining the response of multiple transmitters as a sort of tomographic solution with better resolution of material boundaries in support of new studies, instrument development, and testing.

Summary of Findings to Date

As expected, the vertical extent of an apparent conductivity "pulse" is largely governed by the detection of sea water which has a material conductivity that is roughly an order of magnitude larger than sea ice. However, based on modeled results here, we see a systematic sensitivity to horizontal footprint width in a way that is distinct from traditionally computed 1-D spherical half-space solutions. Specifically,

1) The horizontal extent, and angular variations between, are reaching across the sea ice with a wider footprint developing because of the lower conductivity.
2) When the sea ice is thin (say 1 m), the responding eddy currents are strong between the source and sea water but when the sea ice is thicker, the exponential decay of the response function is much weaker by the time it reaches the sea water such that relative contributions from low conductivity sea ice near the surface begin to equate with sea water that is further away because of the nature of the decaying eddy current strength.
3) Additionally, and more importantly, the footprint area, which is needed for the response function area integration, is not proportional to the distance between the target and the instrument height such that there is a significant variation in instrument footprint even though the instrument may remain at a constant height relative to a reference height such as sea level. In corroboration with the sea ice widening the footprint, the air has an even wider model footprint though a truly negligible conductivity.
4) Hence the conductivity of sea ice, being 10% of the sea water, cannot be neglected like air and snow because of its smaller conductivity weighted by its closer proximity to surface transmitters relative to sea water, specifically in terms of the area integral function over which a relative response is being calculated. Hence, greater care and reconsideration of area integration for response functions is warranted.
5) These findings suggest that footprint width sensitivity could be leveraged to determine ice thickness and/or provide insight into the width of subsurface features through a complementary set of algorithms to the traditional 1-D spherical half-space solutions that currently exist.

Related Papers

(Students Underlined)

Geiger C.A., P. Wadhams, H.R. Müller, J.A. Richter-Menge, J. P. Samluk, T.L. DeLiberty, V. T. Corradina (2015) On the uncertainty of sea-ice isostasy, Ann. of Glaciol., 56(69), doi: 10.3189/2015AoG69A633, http://www.igsoc.org/annals/56/69/

Geiger, C.A., H.R. Müller, E.R. Bernstein, J.P. Samluk, J.A. Richter-Menge (2015) Impact of spatial aliasing on sea-ice thickness measurements, Ann. of Glaciol., 56(69), 353-362, doi: 10.3189/2015AoG69A644 http://www.igsoc.org/annals/56/69/.

Samluk, J.P., C.A. Geiger, and C.J. Weiss (2015) Full-physics 3-D heterogeneous simulations of electromagnetic induction fields on level and deformed sea ice, Ann. of Glaciol., 56(69), 405-414, doi: 10.3189/2015AoG69A737 http://www.igsoc.org/annals/56/69/.

Weiss, C.J. (2013), Project APhiD: A Lorenz-Gauged A-Φ Decomposition for Parallelized Computation of Ultra-Broadband Electromagnetic Induction in a Fully Heterogeneous Earth," Comput. Geosci 58, 40-52 (2013). http://dx.doi.org/10.1016/j.cageo.2013.05.002i